$\delta O_2/N_2$ datasets and gas loss effect

a) Data validation

Table S1 and Table S2 present information about the unpublished and published datasets respectively. Information on the datasets used in Figure 3 can be found in the main body of text in Table 3. Currently no accumulation rate and temperature data for FP and SIR and therefore not included in Figure 3.

Table S1 Information on unpublished datasets used in this study. Core history and measurement information are presented to the best of our knowledge, along with the depth range for each dataset, and the initial form of the gases in the ice: bubble, clathrate, brittle zone (or bubble clathrate transition zone (BCTZ), or mixed. The laboratory at which the measurements were performed, and the method used are stated in the 'Lab' and 'Method' columns, where M-RF stands for melt refreeze method and ME for melt extraction method.

Site	Cored	Measured	Storage T	Lab	Method	Depth	Bubbly or clathrate
	(yr)	(yr)	(°C)			(m)	
BI	2003-2005	2010-2011	-22	LSCE	M-RF	608.85-693.55	BCTZ
EDML	2000-2006	2007	-25	LSCE	ME	596-860	Bubbly
FP	2011-2012	2015	-22	LSCE	ME	289.3-387.75	Bubbly
GISP2	1989-1993	2014	-35	Scripps	M-RF	318.67-1201.22	All
GISP2	1989-1993	2017-2020	-35	Scripps	M-RF	1740.27-2399.45	All
JRI	2008	2011	-22	LSCE	ME	52.25-363.55	Bubbly
NEEM	2008-2012	2011	-20	LSCE	M-RF	1757.25-2524.5	Clathrate
SIR	2018-2019	2021	-22	LSCE	ME	299.75-436.15	Bubbly
TALDICE	2005-2007	2008	-20	LSCE	ME	1003-1291	Clathrate
TALDICE	2005-2007	2009	-20	LSCE	ME	617.48-1401.92	All
TALDICE	2005-2007	2010	-20	LSCE	ME	582.48-902.93	Bubbly and BCTZ
TALDICE	2005-2007	2011	-20	LSCE	ME	1334.92-1550.92	Clathrate
TALDICE	2005-2007	2012	-20	LSCE	ME	1338.95-1553.95	Clathrate
TALDICE	2005-2007	2019	-20	LSCE	ME	1356-1617	Clathrate
TALDICE	2005-2007	2022	-20	LSCE	ME	155-620	Bubbly

Table S2 Information on published datasets used in this study. Core storage history are presented to the best of our knowledge, along with the depth range for each dataset, the initial state of the gases in the ice, and the reference.

Site	Cored (yr)	Measured (yr)	Storage T (°C)	Depth (m)	Bubbly or clathrate	Reference
DF	1993-1996	2006	-50	1204.05-2500.36	All	Kawamura et al., 2007
DF	1993-1996	2017	-50	112.99-2001.06	All	Oyabu et al., 2022
EDC	1999-2004	2005-2008	-50	2483-3188	Clathrate	Landias et al., 2012
EDC	1999-2004	2012	-50	1300 – 1903, 2595 - 3260	Clathrate	Bazin et al., 2016
EDC	1999-2004	2016	-50	1904-2562	Clathrate	Extier et al., 2018
EDC	1999-2004	2021-2022	-50	1489.95 - 1832.6, 1995.95 - 2350.15, 2555.85 - 2633.4, 2744.5 - 2797.85, 2873.75 - 2910.6	Clathrate	Bouchet et al., 2023
GISP2	1989-1993	1993	-35	72.85-2235.05	All	Bender et al., 1994
GISP2	1989-1993	1994	-35	117.7-3032	All	Smith, 1998
GISP2	1989-1993	2006	-35	274.24-2287.88	All	Suwa and Bender, 2008
DE08	2008	-	-	175.15-218.2	Bubbly	Buizert et al., 2020
DSSW20k	1997	-	-	60.88-63.08	Bubbly	Buizert et al., 2020
NGRIP	1996-2004	-	-20	2464.09-2591.69	Clathrate	Bazin et al., 2016
RICE	2011-2013	2015	-36	116-146	Bubbly	Buizert et al., 2020
RICE	2011-2013	2017	-36	60.2-761	Bubbly	Lee et al., 2020
SD	1997-1999	-	-25	69.22-69.66	Bubbly	Buizert et al., 2020
SD	1997-1999	-	-25	74.95-972.98	All	Severinghaus et al., 2009
SP	2014-2016	-	-35	158-188.35	Bubbly	Buizert et al., 2020
SP	2014-2016	-	-35	125.3-1751.01	All	Severinghaus et al., 2019
TALDICE	2005-2007	2020	-20	1350-1600	All	Crotti et al., 2022
VK	1990-1998	2006	-35	174.5-3348	All	Suwa and Bender, 2008
WAISD	2006-2011	2011	-35	80.29-3396.61	All	Severinghaus et al., 2015
WAISD	2006-2011	2015	-35	119.35-190	Bubbly	Buizert et al., 2020

b) GISP2 and TALDICE $\delta O_2/N_2$ data

Successive measurements on clathrate ice shows $\delta O_2/N_2$ depletion through time both from the GISP2 and TALDICE ice cores. A similar effect has been documented at EDC by Bouchet et al., 2023. Interestingly, the 2006 measurements on the GISP2 core clathrate ice (Suwa and Bender, 2008) are comparable to those made more than 10 years earlier (Bender et al., 1994; Smith, 1998). However, there is a depletion of up to 20 ‰ in measurements from between 2017 and 2020 (this study). Data from bubbly ice and within the reported brittle zone shows no gas loss effect.

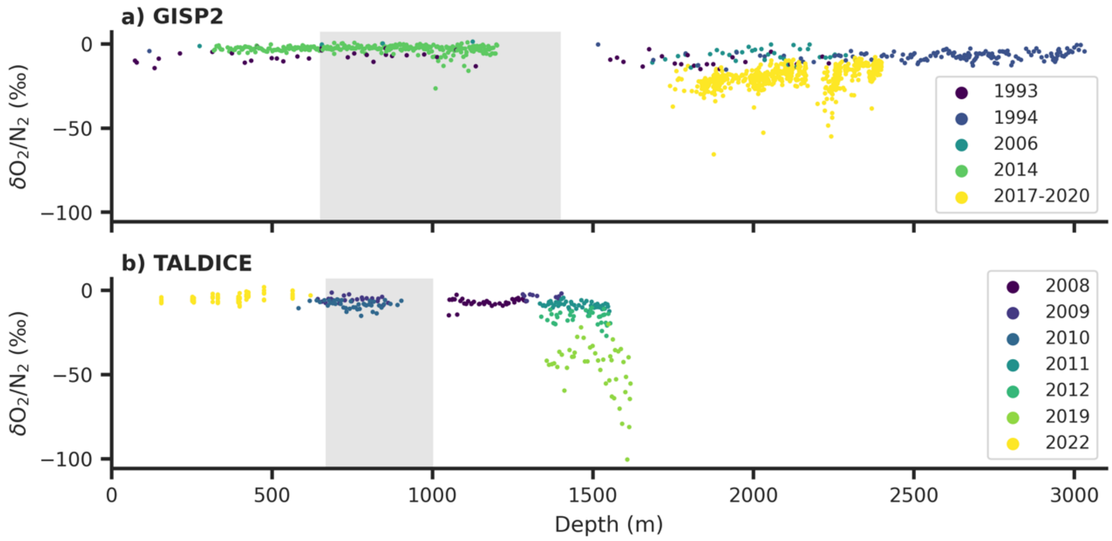

Figure S1 $\delta O_2/N_2$ series from a) the GISP2 ice core and b) the TALDICE ice core after different storage conditions. The years of measurements are indicated and correspond to the different colours of the series. Grey shaded regions represented the reported brittle zones (Neff, 2014).

For the TALDICE ice core, all measurements have been performed on the melt extraction line and storage was only possible at -20°C. Figure S2 is displaying the series of $\delta O_2/N_2$ measured after different periods of storage at -20°C. There is a clear decrease of the mean value of $\delta O_2/N_2$ with storage length at -20°C from 2 years (measurements performed in 2008) to 13 years (measurements performed in 2019) in the clathrate ice. However, we find that the mean value of $\delta O_2/N_2$ in the bubbly ice is still very high even after 16 years of storage at -20°C (mean value comparable to the mean $\delta O_2/N_2$ value for samples measured in 2008) which suggests less or no gas loss for bubbly ice in the TALDICE ice core.

Temporal variability over different time slices from EDC

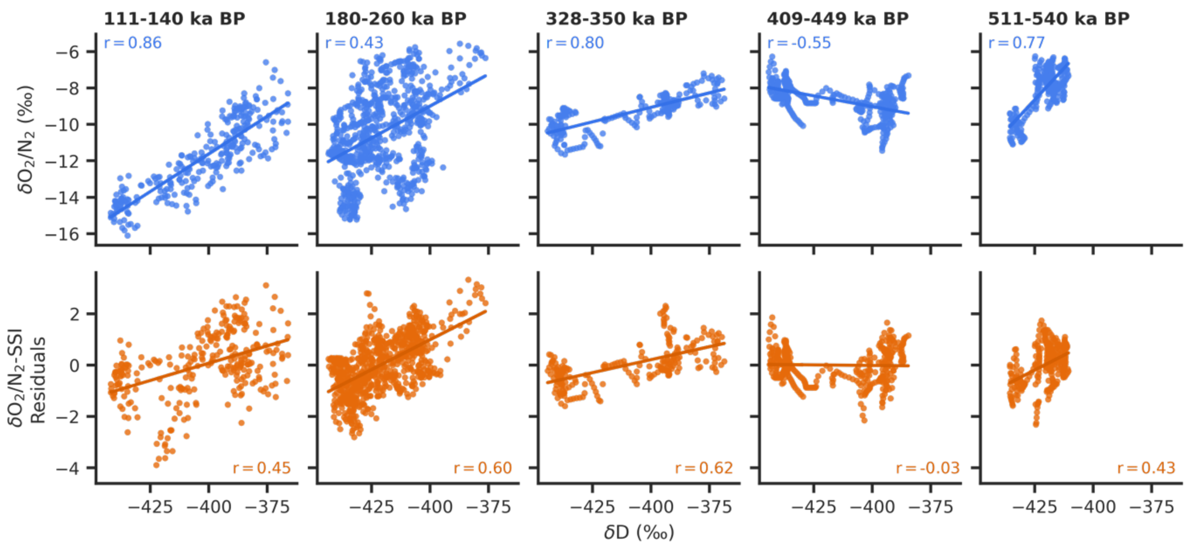

Figure S3 Scatter plots showing each high-resolution section from the EDC core. The upper panel shows the linear regressions between $\delta O_2/N_2$ and δD, and the lower shows the same for $\delta O_2/N_2$ -SSI residuals and δD.

The following section shows that the strong correlation between $\delta O_2/N_2$-SSI residuals and δD during period between 190-260 ka BP are representative the entire core. We run the same analysis as presented in Section 3.1.2 but for the four other sections of high-resolution $\delta O_2/N_2$ measurements from EDC (Bouchet et al., 2023). We observe significant positive correlations between $\delta O_2/N_2$-SSI residuals and δD (and $\delta O_2/N_2$ and δD) for all time periods, except for the period between 409-449 ka BP.

Crocus model temperature evaluation

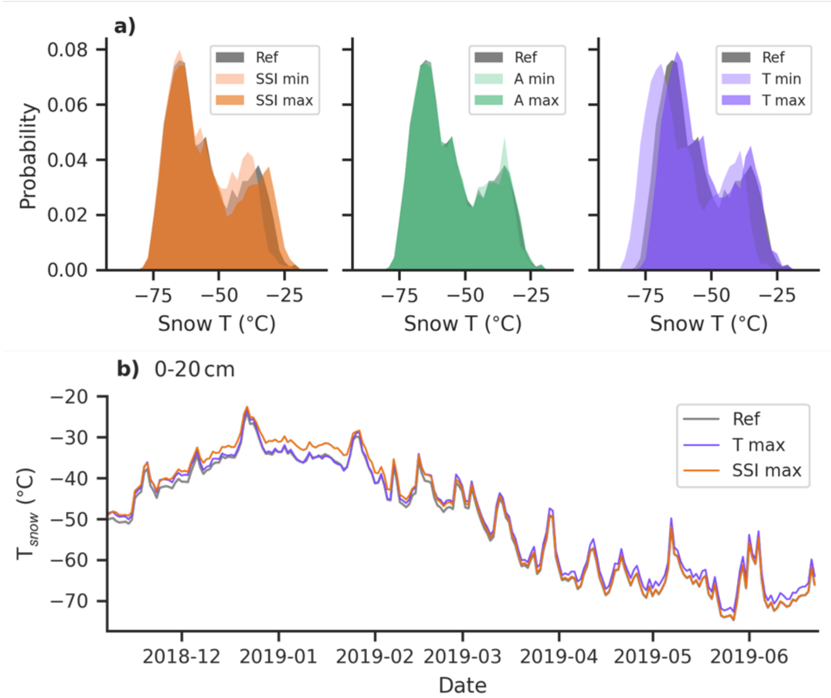

Figure S4 Comparison of simulated snow temperatures in the upper 20 cm at Dome C. Panel a) shows the distributions for each set of simulation; SSI (orange), accumulation rate (green) and temperature (purple) the reference simulation (grey); compared to the reference simulation (grey). A comparison of mean 20 cm snow temperature from the reference (grey), increased temperature (T max), and increase SSI (SSI max) simulations are shown in panel b) between November 2018 and June 2019.

Figure S4 shows the simulated snow temperature distributions over the top 20 cm for the different forcing scenarios. Summer snow temperatures are most sensitive to perturbations in shortwave radiation forcings (SSI), but there is negligible effect in winter due to polar night conditions remaining constant between forcings. Perturbations in accumulation rate appear to have little influence on snow temperature. In contrast, snow temperature is strongly modified by perturbations in air temperature, specifically during winter and in the decreased temperature scenario (T min). Interestingly, the increased temperature scenario (T max) does not substantially influence summer snow temperatures. Figure S4 panel b), showing the daily mean snow temperatures over the top 20 cm, further highlights the non-linear effects of temperature increase where T max results in negligible change in summer temperatures and higher winter temperatures than the reference simulation. As discussed in the main body of text, this is expected to be due to the increased sensitivity of snow temperatures to insolation.

References

Bazin, L., Landais, A., Capron, E., Masson-Delmotte, V., Ritz, C., Picard, G., Jouzel, J., Dumont, M., Leuenberger, M., and Prié, F.: Phase relationships between orbital forcing and the composition of air trapped in Antarctic ice cores, Climate of the Past, 12, 729–748, 2016.

Bender, M. L., Tans, P. P., Ellis, J. T., Orchardo, J., and Habfast, K.: A high precision isotope ratio mass spectrometry method for measuring the O2N2 ratio of air, Geochimica et Cosmochimica Acta, 58, 4751–4758, 1994.

Bouchet, M., Landais, A., Grisart, A., Parrenin, F., Prié, F., Jacob, R., Fourré, E., Capron, E., Raynaud, D., Lipenkov, V. Y., et al.: The AICC2023 chronological framework and associated timescale for the EPICA Dome C ice core, EGUsphere, 2023, 1–39, 2023.

Buizert, C., Baggenstos, D., Bereiter, B., Bertler, N., Brook, E. J., Etheridge, D., et al.: Multi-site ice core Krypton stable isotope ratios, U.S. Antarctic Program (USAP) Data Center. doi: https://doi.org/10.15784/601394, 2020.

Crotti, I., Landais, A., Stenni, B., Bazin, L., Parrenin, F., Frezzotti, M., Ritterbusch, F., Lu, Z.-T., Jiang, W., Yang, G.-M., et al.: An extension of the TALDICE ice core age scale reaching back to MIS 10.1, Quaternary Science Reviews, 266, 107 078, 2021.

Extier, T., Landais, A., Bréant, C., Prié, F., Bazin, L., Dreyfus, G., Roche, D. M., and Leuenberger, M.: On the use of δ18Oatm for ice core dating, Quaternary science reviews, 185, 244–257, 2018.

Kawamura, K., Parrenin, F., Lisiecki, L., Uemura, R., Vimeux, F., Severinghaus, J. P., Hutterli, M. A., Nakazawa, T., Aoki, S., Jouzel, J., et al.: Northern Hemisphere forcing of climatic cycles in Antarctica over the past 360,000 years, Nature, 448, 912–916, 2007.

Landais, A., Dreyfus, G., Capron, E., Pol, K., Loutre, M.-F., Raynaud, D., Lipenkov, V. Y., Arnaud, L., Masson-Delmotte, V., Paillard, D., et al.: Towards orbital dating of the EPICA Dome C ice core using δO2/N2, Climate of the Past, 8, 191–203, 2012.

Lee, J. E., Brook, E. J., Bertler, N. A., Buizert, C., Baisden, T., Blunier, T., Ciobanu, V. G., Conway, H., Dahl-Jensen, D., Fudge, T. J., et al.: An 83 000-year-old ice core from Roosevelt Island, Ross Sea, Antarctica, Climate of the Past, 16, 1691–1713, 2020.

Neff, P. D.: A review of the brittle ice zone in polar ice cores, Annals of Glaciology, 55, 72–82, 2014.

Oyabu, I., Kawamura, K., Uchida, T., Fujita, S., Kitamura, K., Hirabayashi, M., Aoki, S., Morimoto, S., Nakazawa, T., Severinghaus, J. P., et al.: Fractionation of O2/N2 and Ar/N2 in the Antarctic ice sheet during bubble formation and bubble–clathrate hydrate transition from precise gas measurements of the Dome Fuji ice core, The Cryosphere, 15, 5529–5555, 2021.

Oyabu, I., Kawamura, K., Buizert, C., Parrenin, F., Orsi, A., Kitamura, K., Aoki, S., and Nakazawa, T.: DF2021 chronology and Dome Fuji gas data (O2/N2, d15N, CH4) (0 - 207 kyr BP), https://doi.org/10.17592/001.2022061303, 2022.

Severinghaus, J. P.: Nitrogen and Oxygen Gas Isotopes in the Siple Dome and Byrd Ice Cores, Antarctica, U.S. Antarctic Program (USAP) Data Center. doi: https://doi.org/10.7265/N55X26V0, 2009.

Severinghaus, J. P.: Low-res d15N and d18O of O2 in the WAIS Divide 06A Deep Core, U.S. Antarctic Program (USAP) Data Center. doi: https://doi.org/10.7265/N5S46PWD, 2015.

Severinghaus, J. P.: South Pole (SPICECORE) 15N, 18O, O2/N2 and Ar/N2, U.S. Antarctic Program (USAP) Data Center. doi: https://doi.org/10.15784/601152, 2019.

Smith, M.E.: The Pleistocene O2 Record in Two Ice Cores, Senior thesis, Princeton University, Princeton, NJ, 1998, 30pp.

Suwa, M. and Bender, M. L.: Chronology of the Vostok ice core constrained by O2/N2 ratios of occluded air, and its implication for the Vostok climate records, Quaternary Science Reviews, 27, 1093–1106, 2008a.

Suwa, M. and Bender, M. L.: O2/N2 ratios of occluded air in the GISP2 ice core, Journal of Geophysical Research: Atmospheres, 113,765, 2008b.